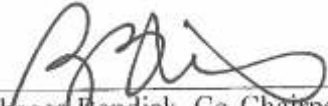


**Innovations in Assessment of Wildfire Effects:
Post-fire Debris Flows and Wildfire Severity
From Sub-pixel to Landscape Scale**

Doctoral Dissertation Proposal

**Karin Riley
Department of Geosciences
University of Montana
November 4, 2008**

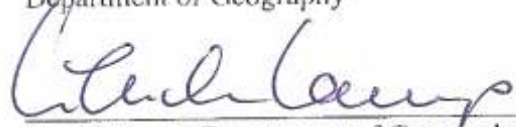
Dissertation Approval Committee



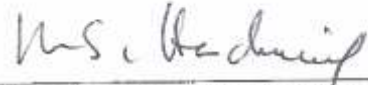
Rebecca Bendick, Co-Chairperson
Department of Geosciences



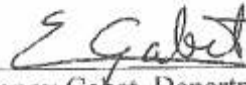
Anna Klene, Co-Chairperson
Department of Geography



Ulrich Kamp, Department of Geography



Marc Hendrix, Department of Geosciences



Manny Gabet, Department of Geology
San Jose State University

Approved by the Department of Geosciences faculty

William Woessner, Department Chair

Date

Table of Contents

Project summary	1
Question 1: Frequency-magnitude distribution of post-fire debris flows	2
Background	2
Methods	4
Study Areas	4
Data	4
Analyses to be performed	5
Question 2: Spatial distribution of fire severity patches and spatiotemporal distribution of fire sizes	5
Introduction	5
<i>Part A: Spectral signatures of burned landscape and evaluation of algorithms for fire severity</i> ..	5
Background	6
Methods	7
<i>Part B: Spatial distribution of fire severity and spatiotemporal distribution of fire sizes</i>	9
Background	9
Methods	10
Study Area	10
Data	11
Analyses to be performed	11
Acknowledgements	11
References	12

Project summary

This project explores the underlying organization of wildfire effects in space and time. The fundamental characteristic of this spatial organization is scale invariance; in other words, phenomena like wildfire and fire-related debris flows show similar patterns at a variety of spatial and temporal scales. Common examples of other scale-invariant phenomena with characteristic noncumulative power-law frequency-size statistics include earthquake- and storm-induced landslides, as well as rainfall and flood events, and earthquakes. This project specifically seeks to quantify simple parameters describing such frequency-size distributions for fire severity patches and post-fire debris flow deposits.

Assessment of the statistical characteristics of fire-related debris flows first requires systematic assessment of the statistical characteristics of fire severity patches. Fire severity itself is a simple metric for gauging fire's effect on the environment, however, problems exist with current algorithms for calculating fire severity from remotely sensed data. The proposed research program therefore also requires development of a spectral tool for assessing fire severity over a range of spatial scales, from the square-meter to landscape.

Using a field spectroradiometer, I collected spectral reflectance measurements of a number of burned and unburned materials including ash, charcoal, mineral soil, charred vegetation, senesced vegetation, and green vegetation. These measurements were collected at two scales, field-of-views (FOV) of 4 cm and of 75 cm. Assumptions about how the reflectances of individual materials aggregate into a single spectral signature at larger scales will be tested using linear spectral unmixing. In addition, algorithms used for assessing fire severity in remotely sensed imagery will be evaluated on the basis of the spectral signatures collected in this study, as well as index theory. If the algorithms are not ideal for assessing fire severity, a new and better-performing algorithm may be written.

Previous studies have documented a strong power-law relationship between fire size and frequency, but such a relationship with fire severity is little studied. The spatial mosaic patterning of fire severity will be investigated by this study using the new fire severity algorithm to generate frequency-area statistics of patch sizes.

Finally, post-fire debris flow statistics will be compiled using a combination of field mapping and existing catalogs. The spatial distributions of fire severity and post-fire debris flows are related in the sense that post-fire debris flows are more likely to initiate in severely burned areas, but the exact frequency-area distributions are likely not related. The size of post-fire debris flows probably depends on factors that do not determine the size of fire severity patches, including the slope, the distance from the initiation site to ridgeline, the distance from the initiation site to the valley floor, and the time since the last debris flow event.

The research described above will result in three journal articles, each contributing to understanding of the spatial and temporal patterns of fire and its impacts on hydrologic and geomorphologic processes. One paper will address the spatiotemporal distribution of post-fire debris flows. Another will resolve fundamental issues in remote sensing of fire severity based on changes in spectral reflectance due to fire, including an assessment of fire severity algorithms. Based on these results, a third paper will analyze the spatial distribution of patches of fire severity and compare the frequency-area distributions of fire in different vegetation types in western Montana.

The following sections of this proposal give a brief literature review, discussion of the scientific problems, and methodology. The first section addresses questions regarding debris flows, and the second section pertains to the questions regarding fire severity.

Question 1: Frequency-magnitude distribution of post-fire debris flows

- *Which probability distribution function best describes the frequency-magnitude distribution of post-fire debris flows?*
- *How is the spatial distribution of post-fire debris flows related to that of fire severity patches?*
- *What does the frequency-area distribution signify for hazard prediction?*

Background

High-magnitude episodic events such as debris flows dominate the sediment yield at millennial timescales (Kirchner et al., 2001). Post-fire debris flows in the Rocky Mountains are typically triggered by short-duration intense rainfall events during the first few years following a fire (Cannon et al., 2001; Cannon et al., 1998; Cannon and Reneau, 2000; Conedera et al., 2003; Parrett et al., 2004). Debris flows are differentiated from landslides in that they are partially or completely liquefied by high pore-fluid pressures (Iverson et al., 1997), and are distinct from fluidized flows in that their behavior can be approximated as a Bingham plastic, which does not deform until it exceeds a threshold shear stress (Lowe, 1979). Simple one-phase rheological models, however, are inadequate for describing debris flow motion; two-phase models that can account for solid-fluid interactions better convey their steep rocky snouts and nearly liquefied tails with elevated pore pressures (Iverson, 1997). Debris flows create a diversity of habitats by introducing a rapid flux of grains of various sizes to streams (Hoffmann and Gabet, 2007), as well as large woody debris (May and Gresswell, 2004).

Post-fire debris flows can cause human catastrophes, and have crossed interstate highways, swept vehicles into rivers, and resulted in serious injuries to motorists (Cannon et al., 1998). Delineation of areas at risk for large debris flows can reduce public hazard. The probability of a debris flow of a certain size can be estimated by parameterizing the frequency-magnitude distribution of past events, taking recent fire history into account. This project proposes to further fundamental understanding of the spatial and temporal organization of wildfire severity and post-fire debris flows in order to enable such forecasts.

The relationship between post-fire debris flows and fire severity has been documented by a number of studies. Post-fire debris flows are more likely to originate in basins with high or moderate fire severity (Gartner et al., 2008). Many factors contribute to post-fire increases in debris flows, including loss of root strength due to plant mortality, reduction of evapotranspiration, increase in runoff due to reduction of storage in canopy and duff, and decrease in infiltration rates due to hydrophobicity of soils, swelling of carbon and inorganic particles, and filling of soil interstices by fine ash particles (Balfour, 2007; Gabet, 2003; Shakesby and Doerr, 2006; Wondzell and King, 2003).

Debris flows initiate by one of three processes. The classic mechanism for debris flow initiation is Coulomb failure, which occurs when the driving stresses exceed the resisting stresses along a plane of failure (Iverson, 1997; Iverson et al., 1997; Ritter et al., 2006). Gravity is the driving stress acting to move sediments downslope, while the resisting stress is provided by the shear strength of the material, a combination of cohesion, the effective normal stress, and the material's overall frictional characteristic, which is commonly expressed as the angle of internal friction. This process is driven by infiltration of rainfall and saturation of the soil, which reduces the resisting stress (Iverson, 1997; Ritter et al., 2006). This mechanism is dominant in the Pacific Northwest, where rainfall events tend to be less intense and longer-duration, allowing for saturation of the soil (Wondzell and King, 2003).

Several studies based on field observation suggest that this mechanism is not the primary one in the case of post-fire debris flows in some regions, including the Interior West, because a clear head scarp is often lacking (Cannon et al., 2001; Cannon et al., 1998; Cannon and Reneau, 2000). Post-fire decreases in infiltration rates and increases in both volume and velocity of overland flow due to removal of biomass induce increased erosion, entrainment, and transportation of sediments. Cascades of overland flow cause failures in colluvium by a second mechanism for post-fire debris flow initiation known as the "firehose effect" (Larsen et al., 2006). This mechanism is prevalent in weathering-limited areas with exposed bedrock, such as Utah's Green River.

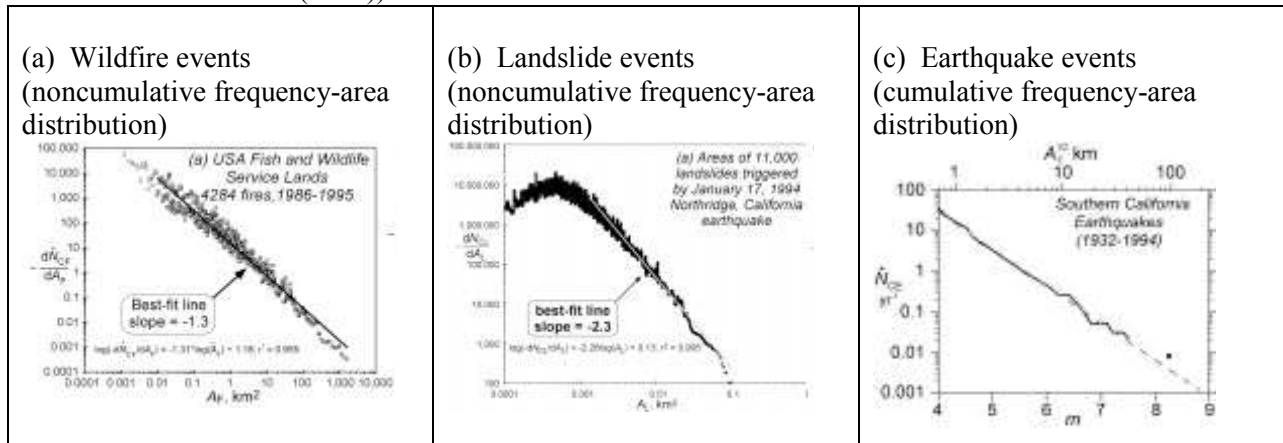
A third mechanism for post-fire debris flow initiation is progressive bulking, a process in which sediment is carried downslope by overland flow, creating a network of rills, which feed sediment into gullies and then larger channels (Wondzell and King, 2003). In the upper reaches of a watershed, the runoff is likely a hyperconcentrated flow, but at some point, the amount of sediment in the flow crosses a threshold to where the grains are supported by grain dispersive pressure transmitted by collisions between grains, or a cohesive matrix of fine sediments rather than fluid; at this point, they are classified as debris flows (Allen, 1997; Cannon et al., 2001; Lowe, 1979). The physics of progressively bulked debris flows have not been well-studied (Richard Iverson and Manny Gabet, personal communication). Progressive bulking is the dominant mechanism for debris flow initiation in the Interior West, where initiation points are often found in colluvial hollows in 0th- or 1st-order streams (Cannon et al., 2001; Wondzell and King, 2003).

Thresholds for post-fire debris flow initiation are often based on the area between the point of initiation and the ridgeline or other topographic barrier, or alternatively on slope angle, rainfall amount and duration (Cannon et al., 2008; Cannon et al., 2001). One study found that the factors showing the strongest correlation with post-fire debris flow volume include slope ($R^2=0.8$) and amount of basin area with high to moderate fire severity ($R^2=0.78$), with these factors being much stronger predictors than lithologic, soil, rainfall and other topography variables ($R^2=0.44$ to -0.67) (Gartner et al., 2008).

Little is known, however, about the frequency-magnitude distribution of debris flow sizes. I hypothesize that the distribution is likely to show power-law behavior, since a number of natural processes including landslides, fires, and earthquakes exhibit a power-law distribution in which small events are much more frequent than large events (Figure 1). Previous work has shown that sizes of landslides follow a noncumulative frequency-area power-law distribution over several scales of magnitude in cellular automata models (Bak, 1990; Bak et al., 1990; Bak et al., 1988; Chen et al., 1990; Malamud and Turcotte, 1999; Paczuski and Bak, 1993; Turcotte and Malamud, 2004) and catalogs of real events (Figure 1b) (Brardinoni and Church, 2004; Chen

et al., 2007; Malamud et al., 2005; Malamud and Turcotte, 1999; Turcotte and Malamud, 2004). Work on debris flows in Europe found much higher occurrences of small debris flows than large ones, but the frequency-magnitude distribution was not parameterized (van Steijn, 1996). In such cases, probability distribution functions can be fit to frequency-magnitude plots of the data, with best-fit lines shown in Figure 1a and 1b. These functions enable prediction of the probability of an event of a certain size occurring during a particular time period, which is useful for risk and hazard assessments (Malamud and Turcotte, 1999).

Figure 1: Power-law behavior in natural hazards, with size of event plotted against frequency (from Malamud and Turcotte (1999))



Methods

Study Areas

Suitable fan deposits in the four following areas will be mapped: 1) the area burned by the Bitterroot Fires of 2000 in the Bitterroot and Sapphire Mountains of southwestern Montana, 2) the area burned by the Moose Fire of 2001 in the North Fork of the Flathead River in northwestern Montana, 3) Myrtle Creek in Idaho, and 4) Yellow Pine in Idaho. Following extensive fires in 2000, a number of debris flows occurred in the Bitterroot Mountains in the Sleeping Child Creek and Laird Creek watersheds, in response to heavy rainfall events (Gabet and Sternberg, 2008; Hyde et al., 2007; Parrett et al., 2004). Rejuvenated gullies have been observed following the Moose Fire, but the deposits have not been examined. Debris flows which followed recent fire events in Myrtle Creek and Yellow Pine in Idaho have been confirmed by colleagues, but are currently unmapped.

Data

During the summer and fall of 2008, I mapped debris flow fans resulting from the fires of 2000 in the Bitterroot and Sapphire Mountains. Watersheds studied include Sleeping Child

Creek, Laird Creek, and the North Fork of Rye Creek. The perimeters of these fans were mapped in the field using high-resolution kinematic GPS.

This and other directly measured data from the northwestern United States will be combined with existing published catalogs of data, including observations from post-fire debris flows in Colorado, Utah, and southern California (Santi et al., 2008), and non-fire-related debris flows in the Alps (van Steijn, 1996).

Analyses to be performed

The area of each debris fan will be calculated for all measured sites. We assume that area is an accurate measure of debris flow magnitude. These new data will be combined with other catalogs described above, appropriately scaled to reflect flow area where observations are currently reported using other measures, such as volume. Finally, the frequency versus magnitude of the debris flows will be plotted, and a power-law rule fitted to the distribution if appropriate.

Fan area will be correlated with basin length to determine how much of the variability in fan area is explained by basin length. Finally, fan area will be correlated with the mean basin fire severity to determine whether fan size depends on fire severity.

Question 2: Spatial distribution of fire severity patches and spatiotemporal distribution of fire sizes

Introduction

Postfire debris flows are related to wildfire severity level as well as presence or absence of fire. However, evaluation of this influence requires accurate assessment of fire severity based on thorough understanding of alterations in spectral reflectance due to fire, which is presently lacking. In order to investigate the spatial relationship of fire severity and postfire debris flow events, I will investigate several fundamental issues with remote sensing of wildfire severity at multiple scales in part A. Applying this information to accurately assess fire severity, in part B, I will analyze the spatial distribution of fire severity patches at the landscape level.

Part A: Spectral signatures of burned landscape and evaluation of algorithms for fire severity

- *What are the characteristic spectral signatures produced by materials commonly found in burned areas of the northern Rocky Mountains and Pacific Northwest?*
- *Which portions of the electromagnetic spectrum are best suited for assessing disturbance due to wildfire?*
- *Using spectral signatures as endmembers, how well does linear spectral unmixing estimate the proportion of unburned and burned materials in satellite imagery?*
- *Which algorithms are best suited for quantifying fire severity?*

- *Can a new algorithm produce a higher correlation with field measures of fire severity level?*

Background

Wildfire severity refers to the degree or magnitude of environmental change caused by fire (Key and Benson, 2006b; Robichaud et al., 2007). The geological and ecological criteria for judging wildfire severity include: chemical and physical changes to soil, conversion of biomass to inorganic carbon, and compositional or structural transformations that create new species assemblages and microclimates. Wildfire severity is dynamic over time during the months following a fire due to survivorship, delayed mortality, and vegetation succession (Key, 2005). In the case of survivorship, vegetation that at first appears dead may in fact remain viable. Conversely, in the case of delayed mortality, vegetation that appears healthy at first may later die due to damage from heat. Both responses can cause fire severity to be over- or under-estimated. Assessment during the first growing season after the fire is more likely to provide a complete and valid representation of severity than assessments performed either earlier or later (Key, 2005).

Fire regimes are divided into three major categories: low-severity, high-severity and moderate-severity (Agee, 1993). In low-severity regimes, frequent fires typically remove understory vegetation but do not cause mortality in large trees. High severity regimes typically experience stand-replacing fires that occur less frequently. Within the moderate-severity regime, also referred to as mixed-severity, both low-severity and high-severity fires occur with varying frequency, and any single fire can incorporate zones of high and low severity. Of the three, the mixed-severity regime is the most poorly understood. Mixed-severity regimes occur predominantly in mid-elevation areas of mixed-conifer forests, where variation in topography creates a complex moisture gradient that results in a mosaic of tree densities and species (Schoennagel et al., 2004). Within all three regimes, a mosaic pattern of different fire severities occurs.

Because of the landscape scale of many large fires, which can extend over 150,000 km² or more, remotely sensed imagery is often used to assess fire severity because it is efficient and cost-effective. The most commonly used methodology involves differencing an algorithm, the Normalized Burn Ratio, which uses the near- and mid-infrared reflectance in a pre- and post-fire image of the burned area (Epting et al., 2005; Kokaly et al., 2007; Miller and Yool, 2002; van Wagtenonk et al., 2004). Of the seven Landsat bands, reflectance values in bands 4 (near-infrared) and 7 (mid-infrared) generally experience the most change from pre-fire to post-fire values, with mid-IR increasing and near-IR decreasing (Key and Benson, 2006b; van Wagtenonk et al., 2004). Previous workers hypothesize that these changes in reflectance are likely due to the removal or charring of vegetation, but spectral evidence is lacking. Instead, performance of the NBR and other fire severity algorithms is evaluated by comparison with the Composite Burn Index (CBI), a field measure of burn severity (Key and Benson, 2006a; van Wagtenonk et al., 2004).

Fundamental questions remain regarding remote assessment of fire severity. In order for a fire severity algorithm to perform ideally, fire severity must be directly related to changes in the reflectance in the spectral region measured by the remote sensor (Roy et al., 2006). In general, fire removes live and dead biomass, converting it to ash and charcoal, or exposing mineral soil. Knowledge of the spectral properties of these materials, which is necessary for evaluation of algorithms, is lacking, with only a few *in situ* spectral signatures in the literature

(Kokaly et al., 2007; Robichaud et al., 2007). To further complicate matters, in most remotely sensed images, a pixel consists of a mixture of several materials, for example green vegetation, soil, and rock. In this case, the pixel's spectrum conveys the sensor's integration of the reflectance curves of several spectrally distinct ground materials.

A technique called linear spectral unmixing (LSU) models reflectance values of mixed pixels as a combination of the reflectance values of the materials found in the pixel. LSU is used to analyze heterogeneous land surfaces (Lu et al., 2002), where each pixel in a remotely sensed image has sub-pixel variability, covering several different ground materials. The component spectral signatures of each material used in the model are referred to as endmembers. LSU uses a system of equations to determine the fractional coverage of each endmember within every pixel, revealing the distribution of a ground material across the landscape (Lewis et al., 2006; Quintano et al., 2006; Robichaud et al., 2007; Rogan and Franklin, 2001). Spectral signatures collected *in situ* at centimeter scales thus can be used as endmembers in LSU and inform interpretation of fire effects at the landscape scale.

The spectral data collected for this project will also be used to evaluate algorithms for fire severity using two methods. 1) The bands used in the fire severity algorithm will be compared to the regions of the electromagnetic spectrum that change most due to a fire event. 2) The change trajectory of the algorithm in spectral feature space will be studied using index theory (Roy et al., 2006).

Methods

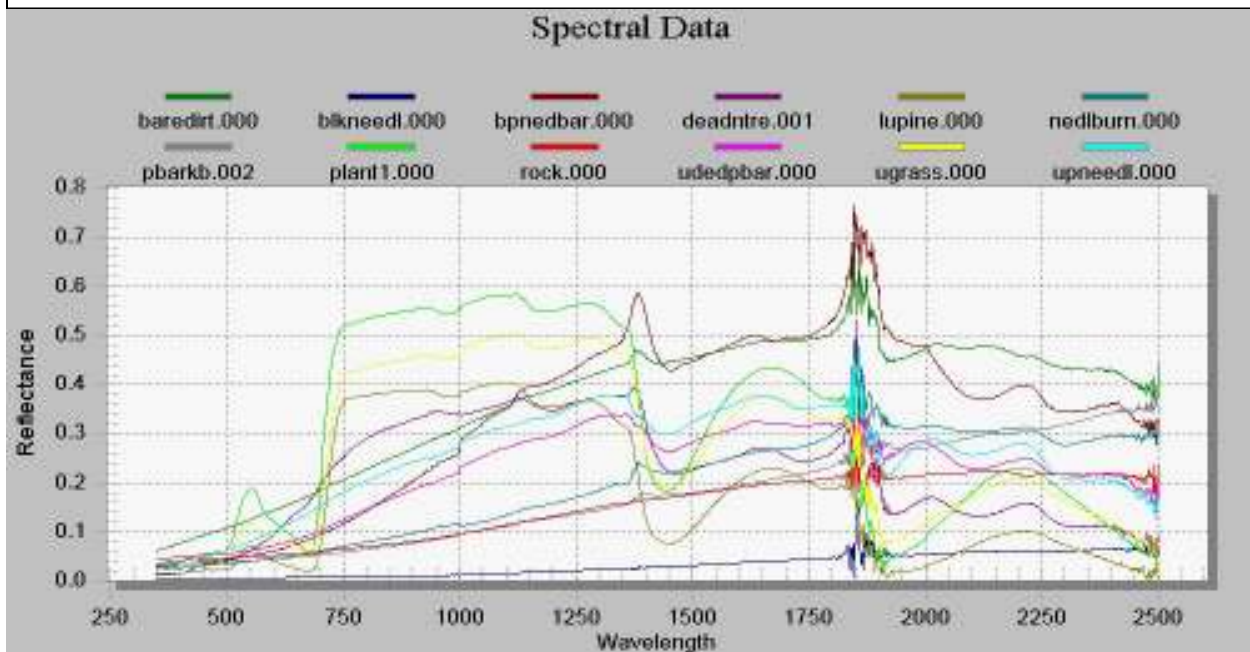
For this project, the FieldSpec3 Spectroradiometer manufactured by Analytical Spectral Devices, Inc. was used to measure sample materials in the field. The instrument measures electromagnetic radiation with wavelengths from 350-2500 nm, with a 2-3 nm sampling interval or spectral resolution. Materials were measured *in situ*, under similar atmospheric and lighting conditions to those experienced by a satellite's sensor.

Spectral reflectance was measured using the FieldSpec3 at several field sites in southwestern Montana during the summer and autumn of 2006 and 2007. Field sites include: 1) the Signal Rock Fire, which burned in the Sapphire Mountains during the summer of 2005, 2) a prescribed fire that burned during April 2006 in the Ninemile Valley, 3) a fire that ignited several acres on Blue Mountain during July 2006, 4) the Gash Creek Fire, which burned several months during the summer and into September 2006, 5) the Bar Fire, a large 2006 fire complex in the Klamath Mountains of northern California, and 6) the Red Eagle Fire, on the east side of Glacier National Park, ignited during the summer of 2006. The Composite Burn Index (CBI) was recorded for each site as a field measure of fire severity. The CBI incorporates estimates of fire severity in the following five structural levels: substrate, herbs and low shrubs, tall shrubs and low trees, intermediate trees, and large trees (Key and Benson, 2006a). Materials commonly found in the burned areas were sampled using the bare fiber optic cable of the spectroradiometer at a distance of approximately 7.5 cm from the sample, a field-of-view of 3.9 cm. A homogenous area of each sample was sought so that the spectral reflectance curve was as close as possible to representing that of the material being sampled with minimal interference from other nearby materials on the ground.

Among the materials sampled using this methodology were: 1) burned materials including ash, charcoal, singed ponderosa pine bark and needles, 2) unburned materials within the burn perimeter, including bare mineral soil, ponderosa pine litter, dry grass, and green

revegetation, and 3) unburned materials outside the burn perimeter including vegetation typical of the area. Data collection was performed on cloud-free days in order to minimize noise from water vapor in the atmosphere. Twenty-five spectra were averaged for each measurement of a sample in order to reduce noise due to fluctuations in the atmosphere. The spectral signatures will be analyzed to determine the potential for distinguishing these materials based on their reflectance properties, especially in the portions of the spectrum represented by satellite bands. Also, portions of the spectrum with the most difference between burned and unburned materials will be identified. Figure 2 shows preliminary results from the Ninemile site. The jagged peak in the data at approximately 1800-1900 nm is due to the presence of water vapor in the atmosphere.

Figure 2. Spectral signatures of materials in a prescribed fire area in the Ninemile Valley. Baredirt = bare mineral soil, blkneedl = blackened needle litter, bpnedbar = blackened burned ponderosa pine needles and bits of bark, deadntre = dead unburned needles of a small standing conifer, lupine = the leaves of a flowering lupine, nedlburn = burned ponderosa pine needle litter, pbarkb = blackened ponderosa pine bark, plant1 = leaf of arnica cordifolia, rock = a grey weathered rock, udedpbar = unburned dead bark of ponderosa tree, ugrass = green grass, upneedl = unburned needle litter



The spectral signatures will be used to make three evaluations. First, they provide endmembers for linear spectral unmixing (LSU). The accuracy of LSU will be tested at two scales: 1) 75.2 cm² field microsites, and 2) 30 m² plots corresponding to Landsat pixels. Ocular estimates of fractional coverage of each endmember in a microsite were recorded in the field, and will be compared with those derived using LSU. At each microsite, spectral measurements were taken approximately 150 cm from the ground, a field-of-view of 75.2 cm. At this distance, the reflectance values of various materials within the field of view are incorporated into a single spectral signature. LSU will be used to estimate fractional coverages of each endmember in the field-of-view, which will be then compared to ocular estimates.

The accuracy of LSU will also be assessed at the pixel scale. Pixels from remotely sensed imagery of study areas will be sampled and unmixed using spectral signatures recorded in

the area. Accuracy will be assessed by comparison with CBI and ocular estimates of fractional coverage of endmembers at each CBI site.

Secondly, the spectral signatures will be used to evaluate the robustness of existing fire severity algorithms based on a theoretical understanding of change in spectral reflectance due to fire. Regions of the spectrum that experience most change during conversion from green vegetation to ash and charcoal will be identified. These regions are most suitable for use in fire severity algorithms.

Thirdly, the spectral signatures will be used to evaluate each algorithm based on index theory. Performance of reflectance values in multispectral space will be tested for all combinations of Landsat TM and ASTER bands.

Part B: Spatial distribution of fire severity and spatiotemporal distribution of fire sizes

Fire size and ecosystem

- *Does the noncumulative frequency-area distribution of wildfire sizes in Montana vary with vegetation type?*

Fire severity

- *How is fire severity distributed across the landscape: randomly, regularly, or clustered?*
- *If it is clustered, do frequency-area distributions of fire severity follow a power-law distribution? If not, what is their distribution?*

Background

Fire size and ecosystem

A number of studies have documented strong power-law relationships in the frequency-area distributions of wildfire sizes in both cellular automata models (Bak, 1990; Bak et al., 1988; Chen et al., 1990; Malamud and Turcotte, 1999; Paczuski and Bak, 1993; Turcotte and Malamud, 2004) and actual events (Malamud et al., 2005; Malamud and Turcotte, 1999). Malamud et al (2005) found robust frequency-area power-law behavior in all 18 Bailey's ecoregions in a coarse-scale analysis of fire regimes in the US. Using a data set of almost 90,000 US Forest Service wildfires from 1970-2000 to calculate probability distribution functions, they estimated fire-return intervals in each ecoregion, and found that large fires were more common in the West. Many vegetation types are lumped into each ecoregion category in their coarse-scale analysis. In this study, a finer-scale analysis will be performed for Montana.

Fire severity

It is not well understood what factors cause spatial variations in wildfire severity, with different studies finding conflicting results with regard to the relationship of wildfire severity to factors such as underlying geology, slope, aspect, elevation, and biomass (Collins et al., 2007; Odion et al., 2004; Rollins et al., 2000; Schoennagel et al., 2004). Rollins et al (2000) found that areas of ponderosa pine and Douglas fir potential natural vegetation burned more frequently than

others in the Selway-Bitterroot Wilderness Area of Idaho and Montana, and in the Gila/Aldo Leopold Wilderness Complex in New Mexico, as did the elevations at which these species assemblages occur. Steep slopes also had higher fire frequencies, but the authors found conflicting signals between the two wilderness areas concerning correlations between fire frequency and aspect. Chafer et al (2004) found an inverse relationship between fire severity and slope, and no relationship with aspect. Collins et al (2007) used biotic (dominant vegetation, time since fire, number of fires) and abiotic (slope, aspect, wind, humidity) variables as explanatory variables in a regression tree analysis for severity of two fires. Their results were contradictory and their models explain only a small amount of variability (12-14% R^2). This failure may be due to lack of inclusion of spatial autocorrelation in fire severity as a factor.

Spatial autocorrelation of fire severity manifests as a mosaic pattern of fire severity patches across the landscape, so modeling the frequency-area distribution of fire severity patches accounts for the presence of spatial autocorrelation. One recent study found a power-law frequency-area relationship in fire severity patches in Montana's Crown of the Continent ecosystem (Rodriguez, 2005). In addition, personal observation in the field has revealed self-similar scale-invariant fractal patterns at several scales: on centimeter scales in moss and litter, on meter scales in a single tree, and at landscape scales in mosaic patterns (Figure 3 and 4).



Figure 3. Mosaic pattern at meter-scale, Signal Rock Fire, Sapphire Mountains, southwestern Montana, summer 2006



Figure 4. Mosaic pattern at landscape-scale, Gash Creek Fire, Bitterroot Mountains, southwestern Montana, summer 2006

Methods

Study Area

Fire size and ecosystem

Western Montana will be the study area for this project.

Fire severity

A sample of at least 35 large fires will be used to assess spatial patches of wildfire severity. Two of these fires will be the Red Eagle Fire in Glacier National Park and the Bar Fire in the Trinity Alps Wilderness of northern California. I have conducted approximately 35 CBI plots in each of these two fires for the purposes of verifying fire severity in remotely sensed imagery.

Data

Fire size and ecosystem

Montana's Natural Resource Information System offers several datasets for vegetation: climax vegetation, ecoregions of Montana, land cover pixels from the GAP Analysis Project at 90 m² scale, and a landcover grid classified from AVHRR at 1 km² scale. One of these three datasets will be used in this study. Fire size and perimeter data is available from the US Forest Service's online FAMWEB database and the Monitoring Trends in Burn Severity (MTBS) website.

Fire severity

Fire severity will be assessed using pre-fire and post-fire Landsat imagery and the best-performing algorithm, as determined in Part B. Post-fire ASTER images were ordered for this project at peak greenness during the summer of 2007 in conjunction with the establishment of CBI plots in the Red Eagle Fire and Bar Fire. Fire severity datasets may also be downloaded from the National Park Service—US Geologic Survey National Burn Severity Mapping Project for large fires classified using the dNBR, or from the MTBS website.

Analyses to be performed

Fire size and ecosystem

For the fine-scale analysis of fire regimes, fire perimeters for US Forest Service, Bureau of Land Management, Bureau of Indian Affairs, and US Fish and Wildlife Service will be downloaded from FAMWEB. These will be loaded into ArcGIS 9.2 along with spatial information on vegetation. Each fire perimeter will be classified according to dominant vegetation type. Frequency-area distributions will be compared for each vegetation type. Fire-return intervals will be determined for each vegetation type.

Fire Severity

In order to confirm that fire severity is indeed clustered rather than randomly distributed, a Ripley's K test will be conducted. Next, each fire severity level will be examined as a separate spatial distribution in a series of binary classifications. For example, unburned and low severity areas will be classified as 0, and moderate and high severity as 1. Areas of all patches will be calculated, and plotted as frequency-area distributions. A probability distribution function will be fit to the data, and a correlation coefficient calculated.

Acknowledgements

Financial support for this project is provided by a 2008 Geological Society of America Research Grant, a 2008 Jerry O'Neal National Park Service Student Fellowship, a 2007 Bertha Morton Fellowship, and a 2007 Clancy Gordon Environmental Scholarship.

References

- Agee, J.K., 1993. Fire ecology of Pacific Northwest forests. Island Press, Washington, DC.
- Allen, P.A., 1997. Earth Surface Processes. Blackwell Publishing, Boston.
- Bak, P., 1990. Simulation of self-organized criticality. *Physica Scripta*, T33: 9-10.
- Bak, P., Chen, K. and Tang, C., 1990. A forest-fire model and some thoughts on turbulence. *Physics Letters A*, 147(5, 6): 297-300.
- Bak, P., Tang, C. and Wiesenfeld, K., 1988. Self-organized criticality. *Physical Review A*, 38(1): 364-374.
- Balfour, V., 2007. The effects of forest fires on runoff rates: The role of duff removal and surface sealing by vegetative ash, Western Montana, University of Montana, Missoula, Montana.
- Brardinoni, F. and Church, M., 2004. Representing the landslide magnitude-frequency relation: Capilano River Basin, British Columbia. *Earth Surface Processes and Landforms*, 29: 115-124.
- Cannon, S.H., Gartner, J.E., Wilson, R.C., Bowers, J.C. and Laber, J.L., 2008. Storm rainfall conditions for floods and debris flows from recently burned areas in southwestern Colorado and southern California. *Geomorphology*, 96(3-4): 250-269.
- Cannon, S.H., Kirkham, R.M. and Parise, M., 2001. Wildfire-related debris-flow initiation processes, Storm King Mountain, Colorado. *Geomorphology*, 39: 171-188.
- Cannon, S.H., Powers, P.S. and Savage, W.Z., 1998. Fire-related hyperconcentrated and debris flows on Storm King Mountain, Glenwood Springs, Colorado, USA. *Environmental Geology*, 35(2-3): 210-218.
- Cannon, S.H. and Reneau, S.L., 2000. Conditions for generation of fire-related debris flows, Capulin Canyon, New Mexico. *Earth Surface Processes and Landforms*, 25: 1103-1121.
- Chafer, C.J., Noonan, M. and Macnaught, E., 2004. The post-fire measurement of fire severity and intensity in the Christmas 2001 Sydney wildfires. *International Journal of Wildland Fire*, 13: 227-240.
- Chen, C.-Y., Fan-Chieh, Y., Sheng-Chi, L. and Kei-Wai, C., 2007. Discussion of landslide self-organized criticality and the initiation of debris flow. *Earth Surface Processes and Landforms*, 32: 197-209.
- Chen, K., Bak, P. and Jensen, M.H., 1990. A deterministic critical forest fire model. *Physics Letters A*, 149(4): 207-210.
- Collins, B.M., Kelly, M., van Wagtenonk, J.W. and Stephens, S.I., 2007. Spatial patterns of large natural fires in Sierra Nevada wilderness areas. *Landscape Ecology*, 22: 545-557.
- Conedera, M. et al., 2003. Consequences of forest fires on the hydrogeological response of mountain catchments: a case study of the Riale Buffaga, Ticino, Switzerland. *Earth Surface Processes and Landforms*, 28: 117-129.
- Epting, J., Verbyla, D. and Sorbel, B., 2005. Evaluation of remotely sensed indices for assessing burn severity in interior Alaska using Landsat TM and ETM+. *Remote Sensing of Environment*, 96: 328-339.
- Gabet, E.J., 2003. Post-fire thin debris flows: sediment transport and numerical modelling. *Earth Surface Processes and Landforms*, 38: 1341-1348.
- Gabet, E.J. and Sternberg, P., 2008. The effects of vegetative ash on infiltration capacity, sediment transport, and the generation of progressively bulked debris flows. *Geomorphology*, 101(4): 666-673.

- Gartner, J.H., Cannon, S.H., Santi, P.M. and Dewolfe, V.G., 2008. Empirical models to predict the volumes of debris flows generated by recently burned basins in the Western U.S. *Geomorphology*, 96: 339-354.
- Hoffmann, D.F. and Gabet, E.J., 2007. Effects of sediment pulses on channel morphology in a gravel-bed river. *GSA Bulletin*, 119(1/2): 116-125.
- Hyde, K., Woods, S.W. and Donahue, J., 2007. Predicting gully rejuvenation after wildfire using remotely sensed burn severity data. *Geomorphology*, 86: 496-511.
- Iverson, R.M., 1997. The physics of debris flows. *Reviews of Geophysics*, 35(3): 245-296.
- Iverson, R.M., Reid, M.E. and LaHusen, R.G., 1997. Debris-flow mobilization from landslides. *Annual Review of Earth and Planetary Sciences*, 25: 85-138.
- Key, C.H., 2005. Remote sensing sensitivity to fire severity and fire recovery. In: J. De la Riva, F. Perez-Cabello and E. Chuvieco (Editors), *Proceedings of the 5th international workshop on remote sensing and GIS applications to forest fire management: fire effects assessment*, Universidad de Zaragoza, pp. 29-39.
- Key, C.H. and Benson, N.C., 2006a. Landscape assessment: ground measure of severity, the Composite Burn Index. In: D.C. Lutes et al. (Editors), *FIREMON: Fire effects monitoring and inventory system*. General Technical Report, RMRS-GTR-164-CD:LA1-LA51. USDA Forest Service, Rocky Mountain Research Station, Ogden, UT.
- Key, C.H. and Benson, N.C., 2006b. Landscape assessment: remote sensing measure of severity: the Normalized Burn Ratio. *FIREMON: Fire effects monitoring and inventory system*. General Technical Report, RMRS-GTR-164-CD:LA1-LA51. USDA Forest Service, Rocky Mountain Research Station, Ogden, UT.
- Kirchner, J.W. et al., 2001. Mountain erosion over 10 yr, 10 k.y., and 10 m.y. time scales. *Geology*, 29(7): 591-594.
- Kokaly, R.F., Rockwell, B.W., Haire, S.L. and King, T.V.V., 2007. Characterization of post-fire surface cover, soils, and burn severity at the Cerro Grande Fire, New Mexico, using hyperspectral and multispectral remote sensing. *Remote Sensing of Environment*, 106: 305-325.
- Larsen, I.J., Pederson, J.L. and Schmidt, J.C., 2006. Geologic versus wildfire controls on hillslope processes and debris flow initiation in the Green River canyons of Dinosaur National Monument. *Geomorphology*, 81: 114-127.
- Lewis, S.A. et al., 2006. Post-wildfire ground cover mapping by spectral unmixing of hyperspectral data, Eleventh Forest Service Remote Sensing Applications Conference, Salt Lake City, UT.
- Lowe, D.R., 1979. Sediment gravity flows: their classification and some problems of application to natural flows and deposits. *Society of Economic Paleontologists and Mineralogists Special Publication*, 27: 75-82.
- Lu, D., Batistella, M. and Moran, E., 2002. Linear spectral mixture analysis of TM data for land-use and land-cover classification in Rondonia, Brazilian Amazon, *Symposium on Geospatial Theory, Processing and Applications*, Ottawa.
- Malamud, B.D., Millington, J.D.A. and Perry, G.L.W., 2005. Characterizing wildfire regimes in the United States. *Proceedings of the National Academy of Sciences*, 102(13): 4694-4699.
- Malamud, B.D. and Turcotte, D.L., 1999. Self-organized criticality applied to natural hazards. *Natural Hazards*, 20: 93-116.

- May, C.L. and Gresswell, R.E., 2004. Spatial and temporal patterns of debris-flow deposition in the Oregon Coast Range, USA. *Geomorphology*, 57: 135-149.
- Miller, J.D. and Yool, S.R., 2002. Mapping forest post-fire canopy consumption in several overstory types using multi-temporal Landsat TM and ETM data. *Remote Sensing of Environment*, 83: 481-496.
- Odion, D.C. et al., 2004. Patterns of fire severity and forest conditions in the western Klamath Mountains, California. *Conservation Biology*, 18(4): 927-936.
- Paczuski, M. and Bak, P., 1993. Theory of the one-dimensional forest-fire model. *Physical Review E*, 48(5): R3214-R3216.
- Parrett, C., Cannon, S.H. and Pierce, K.L., 2004. Wildfire-related floods and debris flows in Montana in 2000 and 2001. In: U.S.G.S. U.S. Department of Interior (Editor). U.S. Geological Survey, Reston, Virginia.
- Quintano, C., Fernandez-Manso, A., Fernandez-Manso, O. and Shimabukuro, Y.E., 2006. Mapping burned areas in Mediterranean countries using spectral mixture analysis from a uni-temporal perspective. *International Journal of Remote Sensing*, 27(4): 645-662.
- Ritter, D.F., Kochel, R.C. and Miller, J.R., 2006. *Process geomorphology*. Waveland Press, Long Grove, Illinois.
- Robichaud, P.R. et al., 2007. Postfire soil burn severity mapping with hyperspectral image unmixing. *Remote Sensing of Environment*, 108(4): 467-480.
- Rodriguez, J.T., 2005. Patch characteristics of post fire landscapes in the Crown of the Continent Ecosystem, Montana, USA, University of Montana, Missoula, MT, 64 pp.
- Rogan, J. and Franklin, J., 2001. Mapping burn severity in southern California using spectral mixture analysis, IEEE 2001 International Geoscience and Remote Sensing Symposium, pp. 1681-1683.
- Rollins, M.G., Swetnam, T.W. and Morgan, P., 2000. Twentieth-century fire patterns in the Selway-Bitterroot Wilderness Area, Idaho/Montana, and the Gila/Aldo Leopold Wilderness Complex, New Mexico. In: U.F. Service (Editor), pp. 283-287.
- Roy, D.P., Boschetti, L. and Trigg, S.N., 2006. Remote sensing of fire severity: assessing the performance of the Normalized Burn Ratio. *IEEE Geoscience and Remote Sensing Letters*, 3(1): 112-116.
- Santi, P.M., deWolfe, V.G., Higgins, J.D., Cannon, S.H. and Gartner, J.E., 2008. Sources of debris flow material in burned areas. *Geomorphology*, 96: 310-321.
- Schoennagel, T., Veblen, T.T. and Romme, W.H., 2004. The interaction of fire, fuels, and climate across Rocky Mountain forests. *Bioscience*, 54(7): 671-676.
- Shakesby, R.A. and Doerr, S.H., 2006. Wildfire as a hydrological and geomorphological agent. *Earth-Science Reviews*, 74(3-4): 269-307.
- Turcotte, D.L. and Malamud, B.D., 2004. Landslides, forest fires, and earthquakes: examples of self-organized critical behavior. *Physica A*, 340: 580-589.
- van Steijn, H., 1996. Debris-flow magnitude-frequency relationships for mountainous regions of Central and Northwest Europe. *Geomorphology*, 15: 259-273.
- van Wageningen, J.W., Root, R.R. and Key, C.H., 2004. Comparison of AVIRIS and Landsat ETM + detection capabilities for burn severity. *Remote Sensing of Environment*(92): 397-408.
- Wondzell, S.M. and King, J.G., 2003. Postfire erosional processes in the Pacific Northwest and Rocky Mountain regions. *Forest Ecology and Management*, 178: 75-87.